Tabassum et al. EURASIP Journal on Wireless Communications and Networking (2016) 2016:2
DOI 10.1186/s13638-015-0494-z

EURASIP Journal on
Wireless Communications and Networking
a SpringerOpen Journal

RESEARCH Open Access

Interference-aware high-throughput channel allocation mechanism for CR-VANETs

Madiha Tabassum[1], Md Abdur Razzaque[1*], Mohammad Mehedi Hassan[2], Ahmad Almogren[2] and Atif Alamri[2]

Abstract

The incorporation of cognitive radio (CR) technology in vehicular ad hoc networks (VANETs) has given birth to a new network, namely CR-VANET, which facilitates the vehicular network to achieve communication efficiency in many resource-demanding applications including video and audio streaming, collision warning, gaming, etc. One of the primary challenges in this CR-VANET network is to allocate high-throughput licensed channels to the application requests in face of interference between the primary users (PUs) and the secondary users (SUs) and among the SUs on the channels. In this paper, we address the channel allocation problem in CR-VANET with the objective of system-wide throughput maximization while maintaining the application quality-of-service (QoS) requirements in terms of channel throughput and packet delivery delay for data transmission. We develop conflict graphs of link-band pairs to describe the interference relationship among source-destination vehicle pairs on different channels and determine independent sets of vehicle pairs that can communicate simultaneously to maximize the spatial reuse of the licensed channels. Finally, we formulate a high-throughput channel allocation problem as a mixed-integer linear programming (MILP) problem. Through extensive simulations, we demonstrate that the proposed interference-aware high-throughput channel allocation mechanism (HT-CAM) provides with better network performances compared to state-of-the-art protocols.

Keywords: CR-VANET, Spatial reusability, Throughput, Channel utilization, Mixed-integer linear program

1 Introduction

The increasing number of on-road vehicles, their use of smart devices, and significant rise in vehicular applications and services, especially in urban environments, have resulted in an overlay crowded dedicated short-range communication (DSRC) spectrum in the 5.9-GHz band. This spectrum scarcity causes degraded vehicular communication efficiency for safety applications (e.g., collision warning, road traffic reporting), bandwidth demanding real-time multimedia (e.g., video and audio streaming), and other legacy applications (e.g., email, web surfing, and so on) [1–5]. However, the spectrum utilization measurements over the past few years indicated a notable number of unused and underused licensed spectrum bands over different space and time. According to the Federal Communications Commission (FCC), temporal and geographical variations in the utilization of the assigned spectrum range from $15 \sim 85\,\%$ [6]. Thus, the licensed bands have now opened by the regulatory agencies such as FCC for opportunistic use by the unlicensed or secondary users (SUs) to increase the utilization efficiency of the available spectrum bands [6–10]. The SUs use the licensed bands through the use of cognitive radio (CR) technology. The CR is an emerging technology to improve spectrum usage and to alleviate spectrum scarcity by exploiting underutilized spectrum resources through opportunistic spectrum access without intercepting the legal or primary users (PUs) of the certain portion of the spectrum.

The growing spectrum-scarcity problem is further intensified due to the augment of high-bandwidth multimedia applications for in-car entertainment, driver-support services, intelligent transportation, etc. These demands have driven the use of CR technology in vehicular environment. The CR technology in vehicular ad hoc network (VANET) enables the vehicles to

*Correspondence: razzaque@du.ac.bd
[1]Green Networking Research (GNR) Group, Department of Computer Science and Engineering, University of Dhaka, Dhaka, Bangladesh
Full list of author information is available at the end of the article

use underutilized licensed bands (e.g., TV white space, GSM white space, and so on) opportunistically. Hence, it improves vehicular communication efficiency by facilitating more efficient radio spectrum usage. In CR-VANETs, each CR-enabled vehicle is equipped with an OBU that has moderate computing and communication capabilities with the entire neighbor vehicles as well as the RSU for Internet accessibility, information sharing, and many other intelligent applications [7]. In such a network, each CR-enabled vehicle needs to implement spectrum management functionalities to (1) detect vacant spectrum opportunities, (2) decide the channel to use based on the quality-of-service (QoS) requests of the applications, and (3) transmit on it but without causing any harmful interference to the licensed owners of the spectrum. Hence, an efficient channel allocation mechanism is of great importance for a CR-enabled vehicle to opportunistically utilize the available licensed spectrum bands. One of the key challenges in this domain is how to perceive higher throughput for CR-enabled on-board devices in vehicles through dynamic access to the available licensed spectrum in the presence of interferences from PUs as well as SUs on different channels.

Although the opportunistic channel access mechanisms for CR networks [11–13] and VANETs [14–17] have been extensively studied in separate, the research in the context of CR-VANET is still at a preliminary stage. The opportunistic channel allocation mechanism in CR-VANET has been investigated in a few number of existing works in the literature [18–21]. A cluster-based optimal channel access framework is proposed in [18], with an objective of maximizing the utility of data transmission by vehicles in a cluster under QoS constraints and collision probability with licensed users. In [19], authors propose a game-theoretic spectrum access scheme for vehicles to opportunistically access licensed channels in a distributed manner where the spectrum access process is modeled as a non-cooperative congestion game. However, these studies fail to achieve maximum possible throughput of the network due to the fact that they deal with individual vehicles to allocate a better channel instead of exploring how to achieve an optimal mapping for the allocation of the available channels to the requested users.

Authors in [20] propose a throughput-efficient channel allocation framework for multi-channel cognitive vehicular networks with the objective of system-wide throughput maximization. A centralized two-step scheme for the spectrum resource allocation is developed in [21] to improve system efficiency and fairness. However, none of the above studies consider spatial reusability [22] of licensed channels for allocating those among non-interfering OBU pairs which can highly improve the overall network throughput as well as the white space utilization.

High vehicular density and mobility and spatial and temporal usage variation of licensed channels by PUs and SUs cause the problem of high-throughput channel allocation in CR-VANET a challenging one. In this work, we propose a novel interference-aware high-throughput channel allocation mechanism for CR-VANET, namely HT-CAM, that focuses on interference-free reusability of licensed channels to maximize the network throughput while the user QoS requirements are met in terms of channel bandwidth and data delivery delay. To cope with the rapidly changing vehicle locations, HT-CAM employs dynamic channel allocation approach at each RSU, which allocates available licensed channels to requested OBU pairs at each scheduling cycle.

In HT-CAM, the number of simultaneous CR transmissions is maximized, i.e., the channel reusability is enhanced with the objectives of maximizing system-wide throughput as well as white space utilization. To achieve this, the HT-CAM develops conflict graphs of link-band pairs to describe the interference relationship among vehicle pairs and determines independent sets of vehicle pairs that can communicate simultaneously. That is, the HT-CAM optimally assigns available channels to the vehicle pairs that want to communicate in a scheduling cycle such that network-wide throughput is maximized, rather exploring an individual vehicle's achievable throughput. We formulate a channel assignment problem as a multi-constraint linear programming problem. The contributions of this paper are itemized as follows:

- A novel interference-aware high-throughput channel allocation mechanism, HT-CAM, has been proposed.
- Interference-free maximum independent sets of link-band pairs have been constructed exploiting conflict graphs so as to maximize the spatial reusability of licensed channels.
- A mixed-integer linear programming (MILP) optimization function is formulated which maximizes network throughput while maintaining QoS requirements of vehicular applications in terms of channel bandwidth and data delivery delay.
- The performance of HT-CAM is simulated extensively and compared with the state-of-the-art channel allocation mechanisms using NS-3.

The rest of the paper is organized as follows. In Section 2, we discuss the existing work on the issue of channel allocation mechanisms in CR-VANET. Subsequently, we present the network model and assumptions used by our mechanism in Section 3. In Section 4, the proposed mechanism is presented in detail, followed by the performance evaluation using NS-3 in Section 5. Finally, we conclude the paper in Section 6.

2 Related works

Channel allocation problem constitutes an interesting and well-investigated research issue of CR networks and VANETs. There are many channel allocation mechanisms proposed for general-purpose CR networks and VANETs which cannot be directly applied to CR-VANETs. This is because the unique features of both vehicular environment and cognitive radio network need to be taken into account while designing the spectrum management mechanisms for CR-VANETs. Despite the significant number of channel allocation mechanisms for VANETs [14–17] and CR networks [11–13, 23], a very few works have been done in the context of CR-VANETs.

In [18], Niyato et al. investigated the optimal channel access in a cluster-based CR-VANETs to maximize the utility of vehicles in a cluster under certain QoS constraints for a grid-like urban street layout, under the assumption that the channel availability statistics are known by the vehicles. In [19], authors studied the channel availability for CR-VANETs in urban scenarios, taking the mobility pattern of the vehicles into account. Exploiting the statistics of licensed channel availability, a distributed opportunistic spectrum access scheme that is based on a non-cooperative congestion game is proposed. However, these methods focus on allocating optimal channel to a vehicle pair requesting transmission that maximizes the throughput of that particular transmission but fails to maximize the aggregated throughput of the network. Hence, new channel allocation mechanisms are needed for network-wide throughput maximization.

In [20], authors proposed a centralized channel allocation framework for system-wide throughput maximization in CR-VANETs. They consider high vehicular mobility, spatial-temporal variations of licensed channels as well as collision probability constraints imposed by the PUs. They developed a probabilistic polynomial time algorithm based on linear programming in order to maximize overall network throughput. The channel allocation decision is taken based on vehicles' packet priorities and packet sizes, expected remaining idle time of each licensed channel.

Authors in [21] considered a centralized CR-VANET architecture where the network is divided into several cognitive cells. A cooperative bargaining spectrum allocation mechanism based on game theory is proposed to formulate the inter-cell and intra-cell resource allocation in CR-VANET with the objective of maximizing system efficiency and fairness.

The existing works allocate channels to the vehicles only considering their interference with primary users. However, none of the existing works have considered the spatial reusability of licensed channels among non-interfering OBU pairs, i.e., they cannot schedule a single channel to more than one non-interfering OBU pairs. Thus, the existing mechanisms do not perform very well when the number of primary users in the network is very high and a very small number of licensed channels are available for opportunistic use. Therefore, we have designed an interference-aware HT-CAM that maximizes overall network throughput by considering spatial reusability of licensed channels. For this purpose, HT-CAM determines independent sets of non-interfering OBU pairs by developing conflict graphs. Finally, HT-CAM develops a linear programming model to obtain the optimal policy for channel assignment to the OBU pairs with objective of network-wide throughput maximization while QoS constraints (e.g., channel bandwidth, data delivery delay) for data transmissions are met.

3 System model and assumptions

We assume a CR-VANET with multiple vehicles, each containing an OBU, opportunisically access vacant licensed channels and an RSU (a base station), which serves a group of on-road vehicles $\mathcal{N} = \{1, 2, 3, \ldots, n\}$, as shown in Fig. 1. The vehicles move on predetermined roads at high speeds and enter/exit the coverage area of an RSU. An OBU is a communication device mounted on vehicles. In CR-VANETs, a vehicles' OBU communicates with other vehicles' OBUs for varieties of applications as mentioned in Section 1. From now on, in this paper, we use the terms "OBU" and "vehicle" interchangeably.

The PU network and the VANET are generally unrelated in terms of communication and services they provide to the customers. While the former uses licensed channels, the latter works on unlicensed channels. In this work, we assume that they co-exist in the same area [6, 7]. We also assume that the arrival pattern of PUs on a channel is Poisson distributed. The OBUs in the vehicles are SUs for the licensed spectrum when no PUs are accessing it.

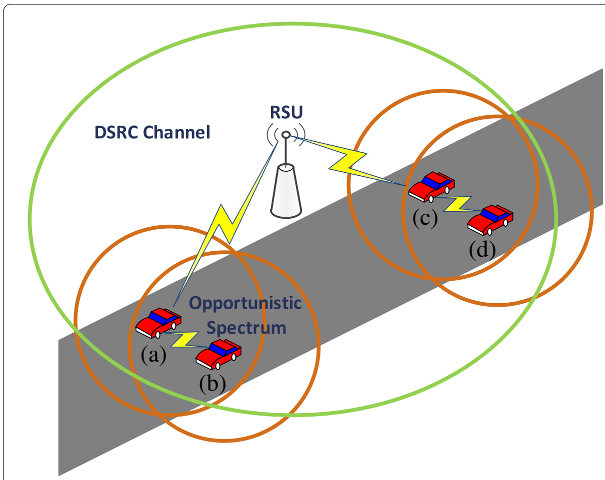

Fig. 1 Network model

In this environment, the OBUs are the CR-enabled SUs of licensed channels. Vacant channels are detected by an individual OBU through periodically running a suitable spectrum-sensing algorithm [24, 25]. Many signal detection techniques can be used for spectrum sensing in order to improve the probability of detection. Existing techniques are categorized as based on energy detection [26], matched filter detection [27], cyclostationary detection [28], and wavelet detection [29]. Any of these techniques can be applicable in our proposed mechanism. Each OBU knows its one-hop neighbor nodes by periodically running neighborhood discovery mechanism, described in Section 4. Each OBU also knows its (x, y) location using GPS.

The list of available licensed channels for an OBU varies over time depending on its location. Let $B = \{1, 2, \ldots, b\}$ be the set of licensed channels, and their bandwidths are $W_1, W_2, \ldots, W_b$, respectively. Let $B_i \in B$ represent the set of licensed channels that are not used by the PUs (i.e., available for opportunistic use), sensed by OBU $i \in \mathcal{N}$, B_i may be different from B_j, where, $i \neq j$, $\forall i, j \in \mathcal{N}$, i.e., possibly, $B_{ij} = B_i \cap B_j = \emptyset$.

In HT-CAM, each OBU has a single transceiver and only single hop communication between source-destination OBUs is considered, no multi-hop communication is allowed. Each OBU has a transmission queue, where data packets are stored temporarily until they are transmitted. We assume that all the data packets in the transmission queue of source OBU i correspond to the same application at a given time and destined to a particular OBU j. Let D_{ij} be the size of the transmission queue, where the length of the data packets in the queue is L_i at a particular time.

The proposed HT-CAM emphasizes on locally available spectrum bands, and, most importantly, the temporal and spatial variations in the PU's channel activities are exploited to determine the optimal allocation of channels. OBUs communicate with each other using one of the available licensed channels decided by the RSU. The communications between an OBU and the RSU are done on the dedicated short-range communication (DSRC) control channel [6, 30]. A transmitter and receiver OBU having a common licensed channel between them can communicate on that channel. Such OBU pairs can be far away from each other and may not be within the interference range of each other. Thus, aforesaid OBU pairs can transmit on the same channel without interfering each-other transmissions. Assume that two OBUs A and C need to send data to the OBUs B and D, respectively, as shown in Fig. 1. Since A and C are not in the interference range of B or D and vice versa, the transmissions at OBU pairs (A, B) and (C, D) on the same channel will not interfere with each other.

In HT-CAM, time is partitioned into equal scheduling cycles with length T. Each scheduling cycle consists of three phases: beacon broadcasting phase, control information reception phase, and channel allocation phase as shown in Fig. 2. In beacon broadcasting phase, RSU broadcasts beacon message containing its identity. This broadcast message is received by all OBUs, helping them to register with RSU for newly arrived OBUs and checking connectivity for the already registered OBUs. Once registered, OBUs that have packets in its transmission queue request the RSU for licensed channels to communicate with the destination OBUs. In the control information reception phase, RSU receives transmission request messages, sensing, and neighborhood information from the OBUs. Finally, in channel allocation phase, the RSU allocates licensed channels to the OBUs by executing

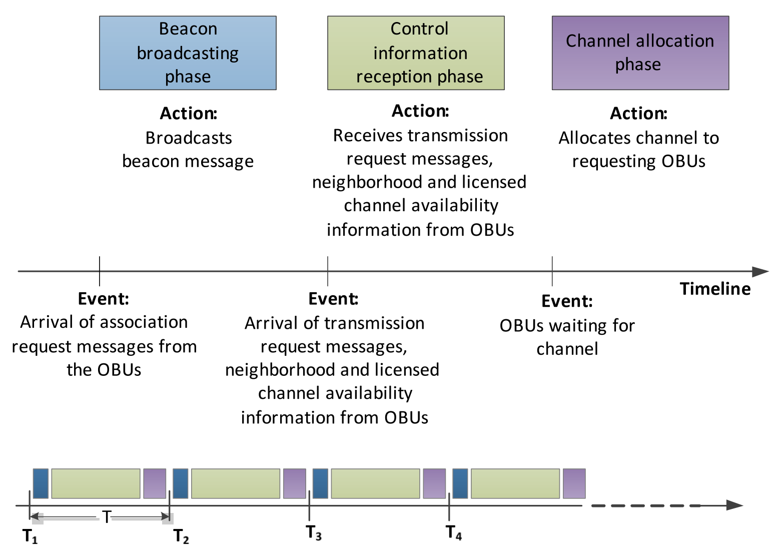

Fig. 2 Scheduling cycle

Table 1 List of notations

Notation	Description
B	Set of licensed channels in the network
W_b	Bandwidth of channel b
$\mathcal{N}$	Set of OBUs registered with an RSU
B_i	Set of available licensed channels at OBU i
B_{ij}	$B_i \cap B_j$, set of common channels available at i and j
T	Length of scheduling cycle
N_i	Set of neighbors of OBU i
P_i^{tr}	Transmission power of an OBU i
D_{ij}	Number of data packets awaited in the queue of OBU i for transmission from OBU i to OBU j
ψ_{ij}	Required data rate for transmission
δ_{ij}	Tolerable maximum transmission delay
Z^b	PU idle time at channel b
λ^b	PU arrival rate at channel b
q_{ij}^b	Transmission quota of OBU pair $\{i,j\}$ on channel b
s_{ij}^b	Success probability of OBU pair $\{i,j\}$ on channel b
R_{ij}^b	Achievable data rate from OBU i to OBU j on channel b
ζ	Medium access delay
SINR_{ij}^b	SINR value between OBU i and OBU j on channel b
L_i	Length of the packets at the transmission queue of OBU i
τ_{ij}^b	Required tx time for OBU pair $\{i,j\}$ on channel b
ρ_l	Weight of independent set l
Θ	Set of all maximum independent sets
$\mathcal{P}$	Set of all OBU pairs requesting transmission
$\mathcal{I}(i)$	Set of OBUs in the interference range of OBU i
$\omega(G)$	Set of all independent vertices in a conflict graph G

our proposed channel allocation mechanism to determine the most suitable channel for a given transmission.

We also assume that each OBU i uses a fixed transmission power P_i^{tr} corresponding to a fixed transmission range and interference range is typically 1.5 to 3 times higher than the transmission range. The notations used to model the problem are listed in Table 1.

4 Design of HT-CAM

In this section, we describe in detail the proposed interference-aware high-throughput channel allocation mechanism, called HT-CAM for CR-VANET. The design components of HT-CAM architecture is shown in Fig. 3. The RSU derives channel preference vectors based on the neighbor discovery and sensing information received from OBUs and generates independent sets by establishing conflict graphs. After that, the RSU assigns weight to each independent set using channel preference vectors. Finally, the RSU selects an independent set such that the

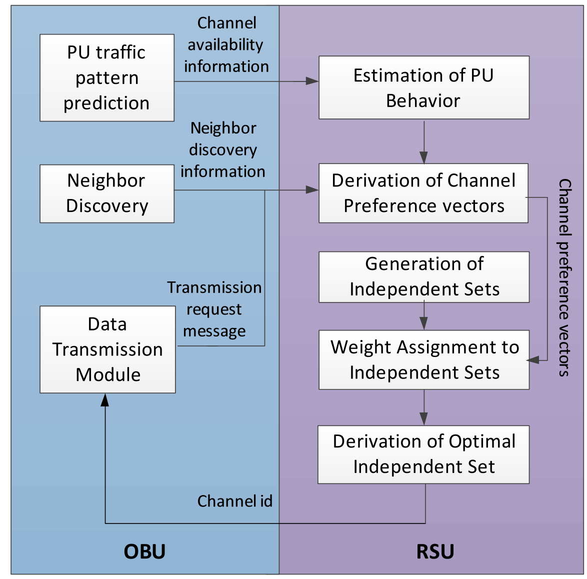

Fig. 3 HT-CAM architecture

network throughput is maximized and assigns channels to OBUs following the channel assignment strategy of the selected independent set.

4.1 Activities of OBUs

OBUs with data packets in transmission queue send request to the RSU for licensed channels. RSU is responsible for allocating communication channels to the OBUs. To facilitate the channel allocation decision at RSU, OBUs need to periodically predict the PU traffic pattern in the licensed channels and send this information to the RSU. OBUs also need to send their neighborhood information to the RSU periodically.

4.1.1 Neighbor discovery

Each OBU maintains a neighbor table. Each neighbor j of i has $|B_{ij}|$ entries in its neighbor table where an entry is structured as $< j, \text{SINR}_{ij}^b >$, where SINR_{ij}^b is the signal to interference plus noise ratio between OBU i and j on license channel $b \in B_{ij}$.

Neighbor discovery is done by each OBU i by periodically broadcasting HELLO message on all the licensed channels in B_i. When an OBU j receives HELLO message from OBU i via a licensed channel $b \in B_{ij}$, OBU j calculates SINR_{ij}^b and enters a new entry $< i, \text{SINR}_{ij}^b >$ in its neighbor table. SINR_{ij}^b is computed as follows [31],

$$\text{SINR}_{ij}^b = \frac{P_{ij}}{P_{\text{noise}} + \sum_{\forall k \in \nu_k^b} P_{kj}} \quad (1)$$

where P_{noise} is the signal strength of Gaussian noise, which is determined depending on the environment, and ν_k^b is the set of all OBUs from which OBU j receives HELLO message on channel b, except OBU i. P_{ij} is the received signal strength from an interfering OBU i at receiver OBU j and is described as follows:

$$P_{ij} = \frac{P_i^{tr}}{||i-j||^{\eta}} \quad (2)$$

where $||i - j||$ stands for the instantaneous distance between OBU i and OBU j and η is the parameter for considering power decay due to distance, and it is usually set between 2 and 4 depending on the environment [32]. Thus, OBUs can easily update their neighbor tables by receiving periodic HELLO messages on their available licensed channels. Afterwards, each OBU performs neighbor discovery and reports its neighbor table to the RSU during control information reception phase in Fig. 2.

4.1.2 PU traffic pattern prediction

All the licensed channels are monitored periodically by the OBUs to assess the communication environment. Through repetitive monitoring of the licensed spectrum, a history of channel usage can be developed. Once a usage history is established, different prediction models (e.g., autoregressive (AR), autoregressive moving average (ARMA) with time varying coefficients, autoregressive integrated moving average (ARIMA), seasonal ARIMA (SARIMA), and so on [33]) can be used to forecast the future PU traffic pattern.

PU traffic pattern prediction enables the OBUs to estimate the licensed channel availability and channel utilization. There are normally two factors considered in the traffic pattern prediction: PU arrival rate and PU idle time. In this paper, OBUs use SARIMA model to predict PU arrival rate and PU idle time. SARIMA model can capture the daily repetitive nature of PU traffic flow and the dependence of present traffic conditions on the immediate past and provide more rational short-term PU traffic flow prediction compared to conventional AR, ARMA, and ARIMA model.

Each OBU i estimates the PU arrival rate, λ_i^b, and PU idle time, Z_i^b, at each of the licensed channels $b \in B$ using SARIMA model according to [34], on the reception of beacon message from the RSU. Afterwards, each OBU i reports a list of PU traffic prediction samples to the RSU. Each sample is structured as $< i, b, \alpha, Z_i^b, \lambda_i^b >$. Here,$\alpha$ is a binary value which represents the availability of channel b to OBU i (0 = PU absent, 1 = PU present).

4.1.3 Transmission request

On reception of beacon message from the RSU, each OBU that has packets on its transmission queue sends a transmission request message, T_{req} to the RSU. Let $\{i,j\}$ be a pair of OBU where source OBU i wants to send packets to the destination OBU j. The source OBU, i of the OBU pair $\{i,j\}$, sends T_{req} message to the RSU. The T_{req} message is structured as $< D_{ij}, P_i^{tr}, \psi_{ij}, \delta_{ij} >$, where D_{ij} is the number of data packets at source i's transmission queue that needs to be transmitted to receiver j, ψ_{ij} is the required data rate for transmission, and δ_{ij} is the maximum data delivery delay that can be tolerated. ψ_{ij} and δ_{ij} are the QoS parameters for a particular transmission. The RSU assigns a channel to the OBU pairs in $\mathscr{P}$ such that these QoS requirements are met. Here, $\mathscr{P}$ is the set of all OBU pairs that sent T_{req} at current scheduling cycle.

4.2 Activities of RSU

The responsibility of an RSU is to allocate the most optimal channel to the requesting OBU pairs. On reception of transmission request messages and sensing information from the OBUs, the RSU computes PU arrival rate (λ^b) and PU idle time (Z^b) for each licensed channel $b \in B$ observed by each user $i \in \mathscr{N}$. After that, it develops two channel preference vectors: *transmission quota* vector, Q_{ij}, and *success probability* vector, S_{ij}, for each pair of OBUs $\{i,j\}$ that wants to communicate (see Section 4.2.2 for details). Then, the RSU solves an optimization problem to maximize overall system throughput by optimal allocation of non-interfering channels to OBU pairs. What follows is to present the details of the RSUs' operation components.

4.2.1 Computation of λ^b and Z^b

Let $\mathscr{Z}^b = \left\{Z_1^b, Z_2^b, \ldots, Z_i^b\right\}$ and $\curlywedge^b = \left\{\lambda_1^b, \lambda_2^b, \ldots, \lambda_i^b\right\}$ be the sets of PU idle times and PU arrival rates, respectively, at channel $b \in B$ sensed by each vehicle $i \in \mathscr{N}$. The RSU first drops the sensing results that are less trustworthy (i.e., results that deviate much from the mean) and updates the sets $\mathscr{Z}^b$ and $\curlywedge^b$ as follows,

$$\mathscr{Z}^b = \left\{Z_i^b \in \mathscr{Z}^b | \quad \left(|\overline{\mu_{\mathscr{Z}}^b} - Z_i^b| \leq \sigma_{\mathscr{Z}}^b\right)\right\}, \quad \forall b \in B \quad (3)$$

$$\curlywedge^b = \left\{\lambda_i^b \in \curlywedge^b | \quad \left(|\overline{\mu_{\curlywedge}^b} - \lambda_i^b| \leq \sigma_{\curlywedge}^b\right)\right\}, \quad \forall b \in B \quad (4)$$

where, $\overline{\mu_{\mathscr{Z}}^b}$ and $\sigma_{\mathscr{Z}}^b$ are the mean and standard deviation of set $\mathscr{Z}^b$, respectively; $\overline{\mu_{\curlywedge}^b}$ and $\sigma_{\curlywedge}^b$ are the mean and standard deviation of set $\curlywedge^b$, respectively. Finally, the RSU computes the mean PU idle time, Z^b, and mean PU arrival rate, λ^b, at each channel $b \in B$ as follows,

$$Z^b = \frac{\sum_{\forall Z_i^b \in \mathscr{Z}^b} Z_i^b}{|\mathscr{Z}^b|}, \quad \forall b \in B \quad (5)$$

$$\lambda^b = \frac{\sum_{\forall \lambda_i^b \in \curlywedge^b} \lambda_i^b}{|\curlywedge^b|}. \quad \forall b \in B \quad (6)$$

These $\mathscr{X}^b$ and λ^b values are used to derive the channel preference vectors, to be discussed in the following subsection.

4.2.2 Derivation of Q_{ij} and S_{ij}

To ensure optimal allocation of available licensed channels to the requesting OBU pairs, the RSU needs to quantify the preference of each channel $b \in B$ in terms of its success probability and availability. The HT-CAM RSU maintains a *transmission quota* vector, Q_{ij}, and a *success probability* vector, S_{ij}, for each OBU pair $\{i, j\}$ based on the computed channel usage statistics, derived in the previous section. We represent Q_{ij} and S_{ij} as 1D column vector of length $|B_{ij}|$, where B_{ij} is the set of common licensed channels between OBU i and j, as shown in Eq. (7). Each entry is corresponding to a specific free data channel $b \in B_{ij}$, i.e., q_{ij}^b and s_{ij}^b represent transmission quota and success probability of OBU pair $\{i, j\}$ on channel b, respectively. In the following, we explain the derivation of column vectors Q_{ij} and S_{ij}.

$$Q_{ij} = \begin{bmatrix} q_{ij}^1 \\ q_{ij}^2 \\ \cdot \\ \cdot \\ \cdot \\ q_{ij}^b \end{bmatrix} \qquad S_{ij} = \begin{bmatrix} s_{ij}^1 \\ s_{ij}^2 \\ \cdot \\ \cdot \\ \cdot \\ s_{ij}^b \end{bmatrix} \tag{7}$$

Transmission quota for an OBU pair $\{i, j\}$, q_{ij}^b, is defined as the maximum number of packets that can be transmitted successfully through a given channel $b \in B_{ij}$ during the interval for which the channel is predicted to be free. Therefore, the upper value of q_{ij}^b is determined by achievable data rate, R_{ij}^b, of a given channel $b \in B_{ij}$ and its PU idle time, Z^b. Therefore, the expression for q_{ij}^b can be written as follows,

$$q_{ij}^b = \min\left\{D_{ij}, \frac{R_{ij}^b \times Z^b}{L_i}\right\} \tag{8}$$

where D_{ij} is the queue size of transmitting node i and the achievable data rate from OBU i to OBU j on channel b, and R_{ij}^b can be calculated using Shannon's capacity equation as follows,

$$R_{ij}^b = W_b \log\left(1 + SINR_{ij}^b\right), \tag{9}$$

where W_b is the bandwidth of channel b, and SINR_{ij}^b is the signal-to-interference plus noise ratio between OBU i and OBU j on channel b, computed in Eq. (1). Hence, the column vector Q_{ij} becomes

$$Q_{ij} = \begin{bmatrix} q_{ij}^1 \\ q_{ij}^2 \\ \cdot \\ \cdot \\ \cdot \\ q_{ij}^b \end{bmatrix} = \begin{bmatrix} \min\left\{D_{ij}, \frac{R_{ij}^1 \times Z^1}{L_i}\right\} \\ \min\left\{D_{ij}, \frac{R_{ij}^2 \times Z^2}{L_i}\right\} \\ \cdot \\ \cdot \\ \cdot \\ \min\left\{D_{ij}, \frac{R_{ij}^b \times Z^b}{L_i}\right\} \end{bmatrix} \tag{10}$$

Now, we derive the column vector S_{ij} for each pair of OBUs $\{i, j\}$ that quantifies the probability that all the awaiting packets in transmission queue (D_{ij}) will be successfully transmitted on each channel $b \in B_{ij}$. The successful transmission probability of OBU pair $\{i, j\}$ on channel $b \in B_{ij}$ without PU interruption is the probability that no PU will appear on channel b during the required transmission period τ_{ij}^b,

$$\tau_{ij}^b = \frac{L_i \times D_{ij}}{R_{ij}^b} + \zeta. \tag{11}$$

where ζ is the medium access delay.

Thus, using Poisson distribution, we can calculate the successful transmission probability, s_{ij}^b, of OBU pair $\{i, j\}$ on channel $b \in B_{ij}$ as follows,

$$s_{ij}^b = e^{-\lambda^b \tau_{ij}^b}, \tag{12}$$

Thus, the column vector S_{ij} becomes

$$S_{ij} = \begin{bmatrix} s_{ij}^1 \\ s_{ij}^2 \\ \cdot \\ \cdot \\ \cdot \\ s_{ij}^b \end{bmatrix} = \begin{bmatrix} e^{-\lambda^1 \tau_{ij}^1} \\ e^{-\lambda^2 \tau_{ij}^2} \\ \cdot \\ \cdot \\ \cdot \\ e^{-\lambda^b \tau_{ij}^b} \end{bmatrix} \tag{13}$$

The channel preference vectors are used to assign weight to the each OBU pair, to be discussed in the following subsections.

4.2.3 Generation of independent sets

In HT-CAM, the RSU first develops a mapping of all possible assignment of the available licensed channels $b \in B_{ij}$ to each requested OBU pair $(i, j) \in \mathscr{P}$, denoted as (ij, b). Then, it finds an independent set I containing only the feasible channel assignments (ij, b) from the map such that no OBU pairs interfere with each other transmissions. In this section, we explain the generation of independent sets in details.

To generate independent sets, the RSU first creates conflict graphs based on the requests received from the OBU pairs $(i,j) \in \mathscr{P}$ and available licensed channels B_{ij} between OBUs i and j. We define a conflict graph $G = (V, E)$, where V is the set of vertices and E is the set of edges; each vertex $v \in V$ corresponds to a link-band pair (ij, b), which indicates that the OBU pair $\{i,j\}$ operates on available licensed channel $b \in B_{ij}$ and the edge set E is constructed in such a way as to represent every interference possibility that can be inferred among OBU pairs in G. Transmissions of two link-band pairs (i_1j_1, b_1) and (i_2j_2, b_2) in G are said to interfere each other if any of the following two conditions holds true:

- *Condition 1*: Two different OBU pairs have at least one common OBU, that is, $\{i_1, j_1\} \cap \{i_2, j_2\} \neq \emptyset$
- *Condition 2*: If two OBU pairs are using the same channel, their transmissions interfere with each other when the transmitter or receiver OBU of one pair falls within the interference range of the transmitter or receiver OBU of the other pair. That is, if there are two channel assignments (i_1j_1, b_1) and (i_2j_2, b_2) such that $b_1 = b_2$, then the transmissions of OBU pairs (i_1j_1, b_1) and (i_2j_2, b_2) interfere *iff* $(i_1) \in \{\mathscr{I}(i_2) \cup \mathscr{I}(j_2)\}$ or $(j_1) \in \{\mathscr{I}(i_2) \cup \mathscr{I}(j_2)\}$ and vice versa. Here, $\mathscr{I}(i)$ is the set of OBUs that fall within the interference range of OBU i.

Based on aforementioned conditions, the RSU connects two vertices $v_1 \in V$ and $v_2 \in V$ of G with an undirected edge $e \in E$, if their corresponding OBU pairs interfere with each other. Let ξ be the set of all possible conflict graphs that can be generated based on the requests received from the OBU pairs $(i,j) \in \mathscr{P}$ and available licensed channels B_{ij} between OBUs i and j, then its size can be calculated as follows,

$$|\xi| = \prod_{\forall (ij) \in \mathscr{P}} |B_{ij}| \tag{14}$$

where $\mathscr{P}$ is the set of all requesting OBU pairs at current scheduling cycle.

Given a conflict graph $G = (V, E)$, we describe the impact of vertex $v_1 \in V$ on vertex $v_2 \in V$, denoted as $\gamma_{v_1 v_2}$ as follows,

$$\gamma_{v_1 v_2} = \begin{cases} 1 & \text{if there is an edge } e \in E \text{ in between } v_1 \text{ and } v_2 \\ 0 & \text{otherwise;} \end{cases}$$

If there is a vertex $v \in V$ in G satisfying the following condition,

$$\sum_{\substack{\forall u \in G \\ u \neq v}} \gamma_{vu} < 1, \tag{15}$$

then transmission at vertex v will be successful even if all the other vertices $u \in V$ are transmitting at the same time. Such a vertex v is called an independent vertex. The RSU updates the set ξ based on the number of independent vertices in the conflict graphs as follows,

$$\xi = \left\{ G \in \xi | \quad (|\omega(G)| = \max_{\forall G \in \xi} |\omega(G)|) \right\}, \tag{16}$$

where $\omega(G)$ is the set of all independent vertices in a conflict graph G. Now, the RSU obtains the updated set ξ using Eq. (16), which contains the conflict graphs having maximum number of independent vertices. The set of all *maximum independent sets* Θ can now be obtained from ξ. The *maximum independent set* is defined as the

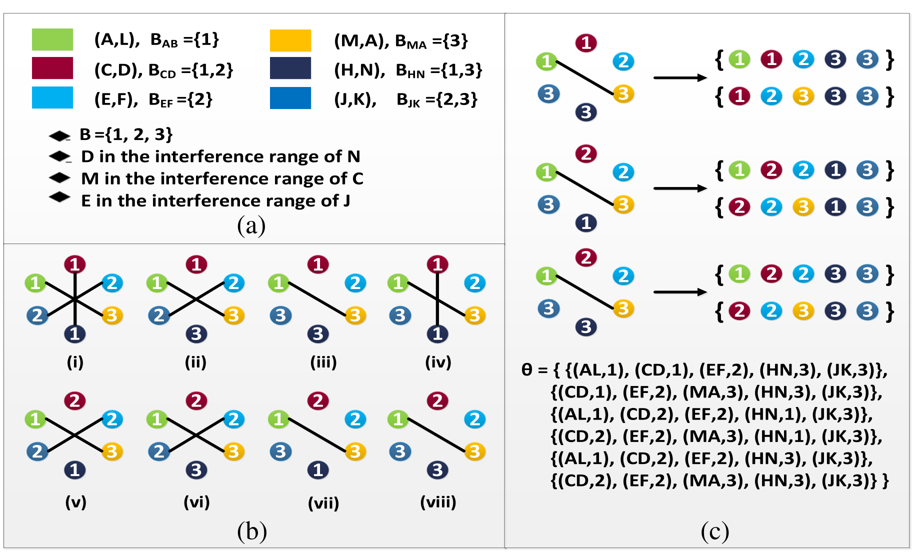

Fig. 4 An illustrative example of generating independent sets. **a** Network scenario. **b** All possible conflict graphs. **c** Generation of Θ

maximum number of vertices in $G \in \xi$ such that each vertex $v \in V$ is an independent vertex. That is, adding any other vertex to the set forces the set to be not independent. The job of RSU is to decide which maximum independent set to choose from Θ.

Here, we provide an illustration of the independent set generation procedure with the help of an example in Fig. 4. The requesting OBU pairs, their common available licensed channels, and the network scenario is shown in Fig. 4a. Figure 4b shows all possible conflict graphs for the scenario of Fig. 4a. Each conflict graph is corresponding to a valid assignment of licensed channels to the requesting OBU pairs. In the conflict graphs, a node is corresponding to an OBU pair (represented by a specific color as shown in Fig. 4a) and the assigned channel to the OBU pair is shown by the channel number associated with each node. In the conflict graph (i), as OBU pairs (A, L) and (M, A) have OBU A in common, their corresponding vertices are connected by an edge in E according to condition 1. Following condition 2, the vertices corresponding to OBU pairs (C, D) and (H, N) are also connected by an edge because they are assigned with the same licensed channel 1 and OBU D is in the interference range of OBU N. There is another edge connected to the vertices corresponding to OBU pairs (E, F) and (J, K) for similar reasons. The RSU takes only the conflict graphs with maximum number of independent vertices. In this case, following Eq. (16), only 3 conflict graphs (iii), (vii), and (viii) are selected by the RSU as each of them have 4 independent vertices. The RSU finds the maximum independent sets for each of the conflict graphs (iii), (vii), and (viii) and develops Θ as shown in Fig. 4c. Θ contains all possible maximum independent sets of a particular scenario.

4.2.4 High-throughput channel allocation

Once we find the maximum independent set Θ, transmission quota vector Q_{ij}, and transmission success probability vector S_{ij}, the problem of high-throughput channel allocation boils down to selecting an independent set from Θ that maximizes the network throughput in a given scheduling cycle, maintaining the QoS requirements of the requesting OBUs. In this subsection, we formulate an LP objective function and the constraints that can solve the required high-throughput channel allocation problem.

In HT-CAM, the RSU assigns a weight ρ_I to each independent set $I \in \Theta$ using the derived channel preference vectors as follows,

$$\rho_I = \sum_{\forall(ij,b)\in I} q_{ij}^b \times s_{ij}^b. \tag{17}$$

Note that higher value of ρ_I is corresponding to high-throughput transmission for the independent set I. Thus, the RSU formulates the mixed-integer linear programming (MILP) problem as follows,

$$\max_{\mathrm{I}} \quad \rho_I, \tag{18}$$

s.t.

$$\forall I \in \Theta \tag{19}$$

$$\tau_{ij}^b \times x_{ij}^b \le Z^b, \quad \forall(ij,b) \in I, \forall b \in B_{ij} \tag{20}$$

$$\sum_{\forall(ij,b)\in I} x_{ij}^b \ge 0, \quad \forall b \in B_{ij} \tag{21}$$

$$R_{ij}^b \ge \Psi_{ij}, \quad \forall(ij,b) \in I \tag{22}$$

$$\tau_{ij}^b \le \delta_{ij}, \quad \forall(ij,b) \in I \tag{23}$$

$$B_{ij} \ne \emptyset, \quad \forall(ij,b) \in I \tag{24}$$

where x_{ij}^b is a boolean variable, $x_{ij}^b = 1$ if OBU pair $\{i,j\}$ is scheduled on channel b, 0 otherwise.

In Eq. (18), the objective is to maximize the weight of independent sets under constraints given in (19–24). The constraint (19) indicates that each independent set is a member of Θ, which is the set of all maximum independent sets. The constraint (20) implies that the idle time of a channel must be greater than or equal to the maximum required transmission time of the OBU pairs scheduled on that channel. The constraint in (21) refers that vehicle pairs can use the same channel simultaneously if their transmissions do not interfere with each other, allowing frequency reuse to achieve better throughput and channel utilization. The constraint in (22) ensures that the achievable data rate of an OBU pair on a channel must be greater than or equal to its required data rate. The constraint in (23) ensures that the delay requirement for data transmission will be met. In (24), the constraint implies that there must be at least one common licensed channel between the source and destination OBU pair. To evaluate the influence of the different parameters on the optimization function, we have used an NEOS optimization tool [35] to solve the MILP problem. Note that, for large number of vehicles and channels, it is an NP-complete problem; however, the constraints (20–24) facilitate us to significantly reduce the input sets in CR-VANET environment and thus the optimal solution was found in polynomial time.

The RSU assigns a channel to the OBU pairs following the assignment strategy of the derived independent set from Eq. (18). Once a channel is allocated to a source-destination OBU pair, the RSU adds that channel to the busy channel set, B_{busy}. As soon as an OBU pair completes transmission on a licensed channel or leaves the transmission range of the RSU, the RSU removes that channel from B_{busy} and marks that channel as free.

5 Performance evaluation

To realize the effectiveness of our proposed HT-CAM, we have used Network Simulator-3 (NS-3) [36] and compared its performances with the state-of-the-art channel selection mechanisms TE-CAM [20] and CC-VANET [21].

5.1 Simulation environment

In our simulation environment, an RSU unit is installed in the middle of a 1000-m road segment where vehicles move with random speeds. First, we have generated the mobility trace of the vehicles using the SUMO tool [37], which is an open-source microscopic traffic road simulation package designed to handle large road networks. The mobility trace file is then imported into the NS-3 tool [36]. For different experiments, we have varied the number of vehicles from 12 to 40, PUs from 3 to 24, and licensed channels from 3 to 10. The data rate of each channel is set to 6 Mbps. The size of each packet is 1024 bytes. Each vehicle runs on the road with a random speed from the range 36 $\sim$ 90 km/h. The transmission ranges of the RSU and OBU are set to 400 and 100 m, respectively. We have defined each scheduling cycle T as 1 s long. Each simulation run lasts for 500 s and the results from 50 simulation runs are averaged for each data points of the graphs. The simulation parameters are listed in Table 2.

5.2 Performance metrics

We compare the performances of the studied channel allocation mechanisms HT-CAM, TE-CAM [20], and CC-VANET [21] based on the following metrics [38].

- *Throughput:* The number of bytes received successfully by each destination node per unit time is measured, and then the average is taken for all destinations to calculate the average throughput achievable by a channel allocation mechanism. Higher value corresponds to better performance.
- *Packet delivery ratio:* It is the ratio of total number of packets successfully delivered at destination nodes to the total number of packets generated during the whole simulation period.
- *Channel utilization ratio:* It is the ratio of the number of scheduled OBU pairs to the number of available licensed channels during the whole simulation period.
- *End-to-end average packet delivery delay:* The end-to-end delay is the time from when a packet becomes head of the line packet to the time when the source receives acknowledgement from the destination for that packet. Then, the average delay is calculated for all packets sent during the whole simulation period. Lower end-to-end delay means better channel allocation mechanism.
- *Operation overhead:* We calculate the amount of control bytes transmitted during the whole simulation period for successful transmission of each byte of user data in the studied channel allocation mechanisms to compare the operation overhead.

Table 2 Simulation parameters

Parameter	Value
Number of vehicles	12 $\sim$ 40
Number of PU	3 $\sim$ 24
Number of channels	3 $\sim$ 10
Channel bit rate	6 Mbps
Data packet size	1024 bytes
ACK size	14 bytes
Control packet size	16 bytes
Channel bit error rate	10^{-3}
Vehicles speed	36 $\sim$ 90 km/h
Vehicle transmission range	100 m
RSU transmission range	400 m
MAC layer model	AdhocWifiMac model
Physical layer model	YansWifi model
Length of road segment	1000 m
Simulation time	500 s

5.3 Simulation results

5.3.1 Impacts of increasing number of PUs

In this section, we measure the aforementioned performance metrics for varying number of primary users ranging from 3 to 24, as shown in Fig. 5. The number of vehicles and licensed channels in the network is set to 24 and 7, respectively.

As the number of PUs increases, all the studied protocols suffer from performance degradation in terms of throughput, as shown in Fig. 5a. We can see that HT-CAM achieves better network throughput than TE-CAM and CC-VANET. This is mainly due to the fact that the HT-CAM considers spatial reusability of licensed channels, i.e., it can schedule a single channel to more than one non-interfering OBU pairs at each scheduling cycle. Moreover, the HT-CAM allocates channels to the requested OBU pairs in such a way that the most optimal channels (in terms of PU activities) are allocated to the maximum possible number of OBU pairs. As a result, more data packets are transmitted successfully to the destination OBUs without experiencing interruptions from primary users, achieving higher throughput.

In the graphs of Fig. 5b, we observe that the packet delivery ratio decreases sharply with the increasing number of primary users in all the studied channel allocation mechanisms. It is also noticed that the proposed HT-CAM is much tolerant to increasing PU arrivals compared to TE-CAM and CC-VANET. The reason behind this result is that the HT-CAM assigns more stable licensed channels in terms of PU arrival rate and PU idle time to more than one requested OBU pairs, if their transmissions do not

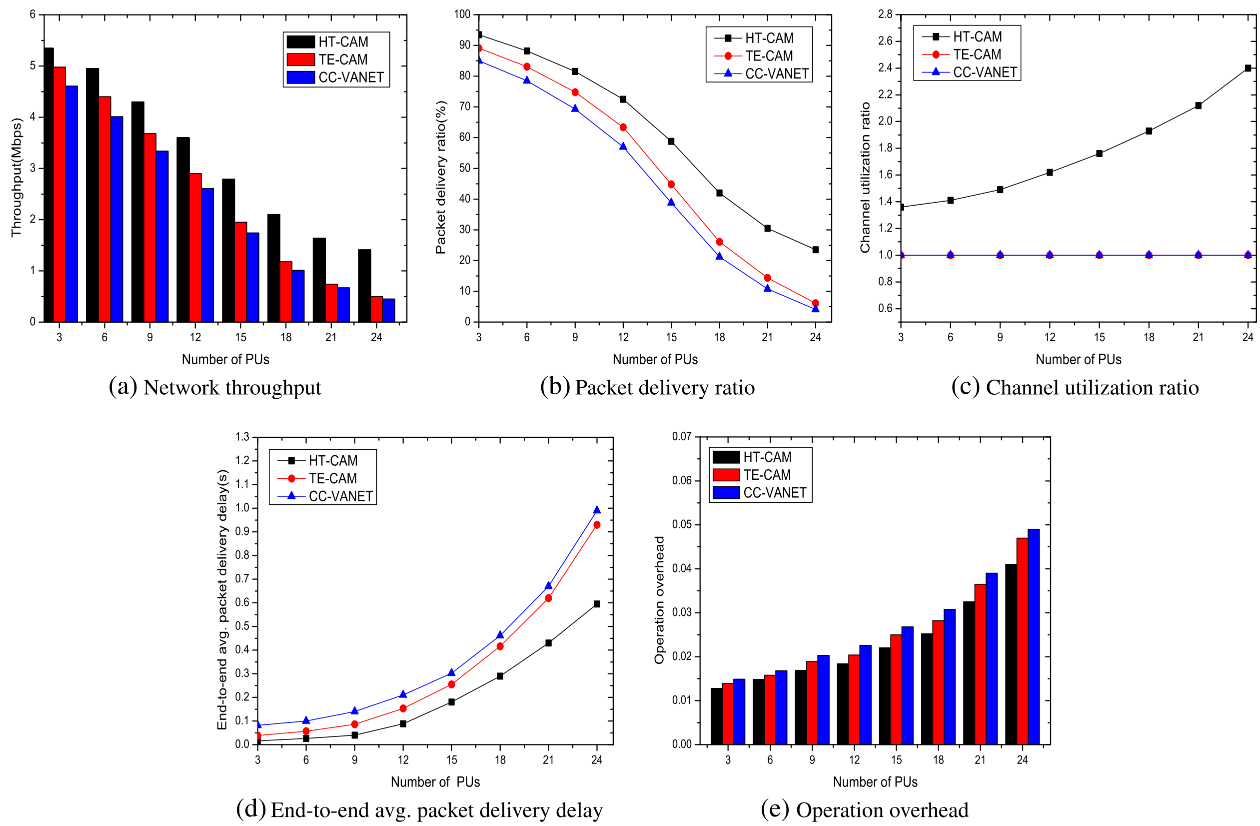

Fig. 5 Impacts of number of PUs. **a** Network throughput. **b** Packet delivery ratio. **c** Channel utilization ratio. **d** End-to-end average packet delivery delay. **e** Operation overhead

interfere with each other. As a result, the chance of PU appearance in the allocated licensed channels is lower in our proposed HT-CAM than that in TE-CAM and CC-VANET. Therefore, the number of packet drops decreases and more data packets are delivered successfully to the destination.

In Fig. 5c, we observe the performance of studied protocols in terms of available licensed channel utilization. When the number of PUs is large in the network, only a small number of licensed channels are available for opportunistic use. The number of requested OBU pairs TE-CAM and CC-VANET can schedule is equal to the number of available licensed channels. Therefore, when the number of available licensed channels is very low in the network, they can allocate only a small number of requested OBU pairs. On the other hand, HT-CAM is able to schedule a much higher number of OBU pairs with limited number of available licensed channels by spatial reuse. Thus, the utilization of available licensed channels increases with increasing number of PUs in the network.

In Fig. 5d, we observe the performance of the studied protocols in terms of end-to-end average packet delay. Note that the end-to-end average packet delay increases sharply as the number of PUs increases in all the studied protocols. The performance of HT-CAM is still better than TE-CAM and CC-VANET because of better channel allocation by HT-CAM and reduced waiting time offered by it. Moreover, in TE-CAM and CC-VANET, the chance of PU appearance in the allocated licensed channels is slightly higher than HT-CAM that results in more packet drops. Thus, the number of packet retransmissions increases, which in turn extends the average end-to-end average packet delay.

In Fig. 5e, we compare the operation overhead of HT-CAM, TE-CAM, and CC-VANET for increasing number of PUs in the network. As the number of PUs increases, the more licensed channels become occupied by them. Thus, the number of scheduled OBU pairs at each scheduling cycle decreases and the number of packet retransmissions increases. As a result, the throughput decreases and the comparative amount of control bytes exchanged increases. These cause the protocol operation overhead to increase with the increasing number of PUs in all the studied protocols. However, the proposed HT-CAM performs better than TE-CAM and CC-VANET because of a higher number of scheduled OBU pairs and lower number of packet retransmissions even in the presence of a large number of PUs in the network.

5.3.2 Impacts of increasing number of vehicles

We study the performances of the studied algorithms for increasing number of vehicles in the network, ranging from 12 to 40, as shown in Fig. 6. The number of PUs and licensed channels in the network is set to 9 and 7, respectively.

The number of vehicles has a great impact on the network throughput. In Fig. 6a, we observe that in all the studied protocols, the throughput reduces as the number of vehicles in the network increases. This happens because the number of requests arriving to the RSU increases with the number of vehicles at each scheduling cycle. But the RSU can schedule only a portion of the requested OBUs because of the fixed number of licensed channels in the network. Initially, when the number of requested OBU pairs is small, all the studied protocols show similar performances. However, as the number of vehicles increases in the network, HT-CAM shows much better performance than TE-CAM and CC-VANET. This is caused by HT-CAM's capability of scheduling more OBU pairs on the licensed channels. Therefore, the throughput performance gap between the HT-CAM and the others increases with the number of vehicles.

In Fig. 6b, we can observe that HT-CAM performs much better than TE-CAM and CC-VANET, in terms of packet delivery ratio with increasing number of vehicles. This happens because HT-CAM can schedule much higher number of OBU pairs at each scheduling cycle than TE-CAM and CC-VANET. Thus, more data packets are received by destination OBUs at each scheduling cycle, which in turn increases the packet delivery ratio in the network.

The utilization of available licensed channels is also affected by the number of vehicles. In Fig. 6c, we observe that, initially when the number of vehicles in the network is small, the channel utilization ratio is less than one for all of the studied mechanisms. The reason behind that is the available licensed channels remain underutilized with small number of requests at the RSU. We can also see that the channel utilization ratio of HT-CAM increases rapidly with increasing number of vehicles, since more OBUs are scheduled by the RSU with fixed number of licensed channels in the network. After a while, the utilization ratio becomes almost stable because only a fixed portion of the vehicles can utilize the licensed channels and any further increment of vehicles does not have much impact on the

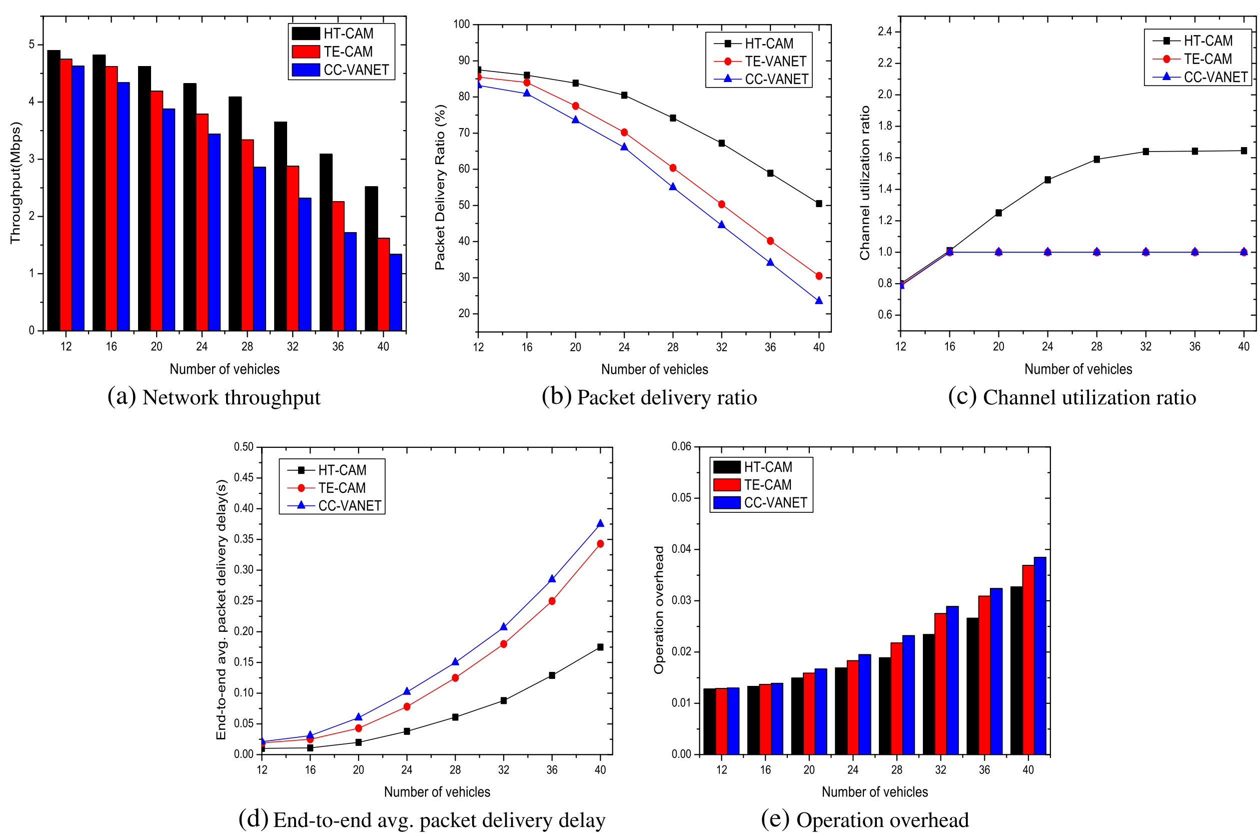

Fig. 6 Impacts of number of vehicles. **a** Network throughput. **b** Packet delivery ratio. **c** Channel utilization ratio. **d** End-to-end average packet delivery delay. **e** Operation overhead

utilization of licensed channels. On the other hand, in TE-CAM and CC-VANET, once the utilization ratio reaches to 1.0, it becomes stable since it cannot reuse the channels.

Figure 6d depicts that the end-to-end average packet delivery delay is much smaller in HT-CAM than TE-CAM and CC-VANET. In TE-CAM and CC-VANET, the number of OBUs transmitted at each scheduling cycle is limited by the number of available licensed channels. Due to their poor resource utilization, the packets spend more time in the transmission queues, increasing the delivery delay. In contrast, HT-CAM can accommodate a much higher number of requests arriving at the RSU and thus it decreases the end-to-end average packet delivery delay.

In Fig. 6e, we observe that the operation overhead increases with the increasing number of vehicles in all the studied protocols as expected theoretically. The proposed HT-CAM performs better than TE-CAM and CC-VANET since it achieves higher amounts of data byte delivery for a little increase in control byte transmissions.

5.3.3 Impacts of increasing number of licensed channels

In this section, we study the performance of the studied channel allocation mechanisms for increasing number of licensed channels in the network ranging from 3 to 10, as shown in Fig. 7. The number of vehicles and PUs in the network is fixed at 24 and 9, respectively.

In Fig. 7a, we can observe that, with the increase of licensed channels, the network throughput increases gradually. But the increment rate is much higher for HT-CAM than both TE-CAM and CC-VANET, because of the spatial reusability mechanism of HT-CAM, which allows more OBU pairs to transmit data packets even if the number of licensed channels in the network is limited. However, at higher number of licensed channels, the throughput of the studied mechanisms comes closer due to the more resource availability compared to the traffic loads.

We observe the performance of studied mechanisms in terms of packet delivery ratio in Fig. 7b. The graphs state that the packet delivery ratio grows rapidly with increasing number of licensed channels for all the studied mechanisms, as expected theoretically. However, the HT-CAM shows better performance than TE-CAM and CC-VANET, especially, when the number of licensed channels in the network is small, caused by spectrum reuse capability of HT-CAM.

Figure 7c depicts that the channel utilization ratio decreases in HT-CAM with increasing number of licensed

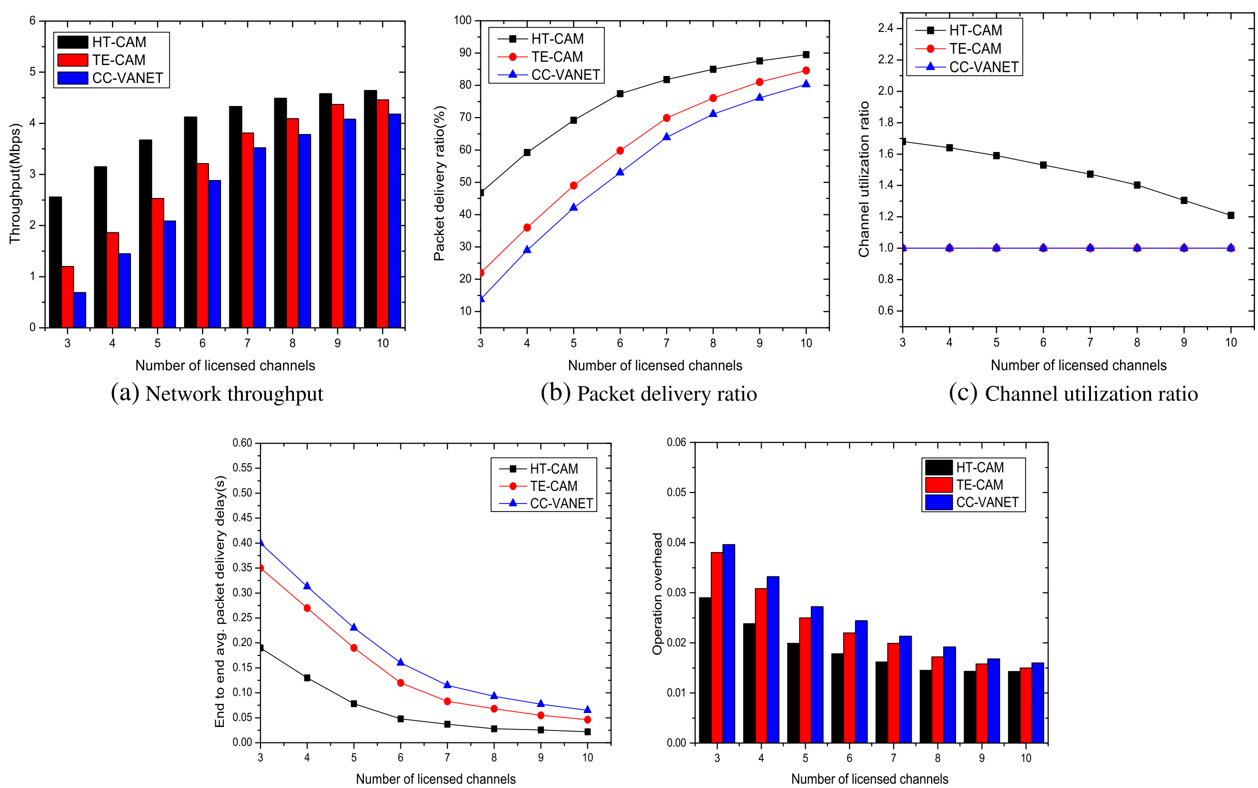

(a) Network throughput (b) Packet delivery ratio (c) Channel utilization ratio (d) End-to-end avg. packet delivery delay (e) Operation overhead

Fig. 7 Impacts of number of licensed channels. **a** Network throughput. **b** Packet delivery ratio. **c** Channel utilization ratio. **d** End-to-end average packet delivery delay. **e** Operation overhead channels in the network. This happens as the number of licensed channels increases the utilization of individual licensed channel reduces. However, the channel utilization ratio of HT-CAM is still higher than TE-CAM and CC-VANET because of the more efficient allocation of licensed channels among the requested OBU pairs.

The graphs of Fig. 7d depict that the end-to-end average packet delivery delay decreases rapidly as the number of licensed channels increases in the network for all the studied protocols. Initially, when the number of licensed channels is very small in the network, HT-CAM shows significant performance improvement than TE-CAM and CC-VANET. The fact behind this is already stated in earlier graphs.

The graphs of Fig. 7e state that the proposed HT-CAM has less overhead compared to TE-CAM and CC-VANET, since the former offers better throughput in cost of little control byte overheads.

6 Conclusions

In this paper, we have developed an interference-aware high-throughput channel allocation mechanism, called HT-CAM, that addresses the unique challenges of CR-VANETs. We create conflict graphs of link-band pairs to extract non-interfering OBU pairs that can communicate simultaneously on a given channel, increasing the spatial reuse of the available channels. The multi-constraint linear optimization technique of HT-CAM helps it to make channel allocation decision more efficient. The results of the simulation experiments, carried out in NS-3, reveal that the HT-CAM outperforms state-of-the-art channel allocation mechanisms for CR networks in terms of network throughput, channel utilization, end-to-end packet delivery delay, etc.

Competing interests

The authors declare that they have no competing interests.

Acknowledgements

The authors would like to extend their sincere appreciation to the Deanship of Scientific Research at King Saud University for its funding of this research through the Research Group Project no. RGP-VPP-281. Special thanks to the ICT Division of the Government of Bangladesh for student fellowship.

Author details

[1]Green Networking Research (GNR) Group, Department of Computer Science and Engineering, University of Dhaka, Dhaka, Bangladesh. [2]College of Computer and Information Sciences, King Saud University, Riyadh 11543, Kingdom of Saudi Arabia.

Received: 29 September 2015 Accepted: 8 December 2015
Published online: 04 January 2016

References

1. MM S Al-Sultan, AH Al-Doori, H Al-Bayatti, A Zedan, Comprehensive survey on vehicular ad hoc network. J. Netw. Comput. Appl. **37**, 380–392 (2014)
2. AM Vegni, M Biagi, R Cusani, *Smart vehicles, technologies and main applications in vehicular ad hoc networks. Vehicular Technologies—Deployment and Applications*, (2013). DOI: 10.5772/55492
3. Y Zeng, K Xiang, D Li, AV Vasilakos, Directional routing and scheduling for green vehicular delay tolerant networks. Wirel. Netw. **19**(2), 161–173 (2013)
4. L Zhou, YZ Song, KW Jing, Distributed media services in P2P-based vehicular networks. IEEE T. Veh. Technol. **60**(2), 692–703 (2011)
5. W Viriyasitavat, M Boban, H-M Tsai, A Vasilakos, Vehicular communications: survey and challenges of channel and propagation models. IEEE Veh. Technol. Mag. **10**(2), 55–66 (2015)
6. KD Singh, P Rawat, J-M Bonnin, Cognitive radio for vehicular ad hoc networks (CR-VANETs): approaches and challenges.EURASIP. J. Wirel. Commun. Netw. **2014**, 49 (2014)
7. MD Felice, R Doost-Mohammady, KR Chowdhury, L Bononi, Smart radios for smart vehicles: cognitive vehicular networks. IEEE Veh. Technol. Mag. **7**(2), 26–33 (2012)
8. S-S Byun, I Balashingham, AV Vasilakos, H-N Lee, Computation of an equilibrium in spectrum markets for cognitive radio networks. IEEE Trans. Comput. **63**(2), 304–316 (2014)
9. V Chakravarthy, X Li, Z Wu, MA Temple, F Garber, R Kannan, A Vasilakos, Novel overlay/underlay cognitive radio waveforms using SD-SMSE framework to enhance spectrum efficiency.Part I: theoretical framework and analysis in AWGN channel. IEEE Trans. Commun. **57**(12), 3794–3804 (2009)
10. M Yang, D Jin, L Zeng, X Wu, AV Vasilakos, Software-defined and virtualized future mobile and wireless networks: a survey. MONET. **20**(1), 4–18 (2015)
11. Z Han, R Zheng, HV Poor, Repeated auctions with Bayesian nonparametric learning for spectrum access in cognitive radio networks. IEEE Trans. Wirel. Commun. **10**(3), 890–900 (2011)
12. O Naparstek, A Leshem, E Jorswieck, *Distributed medium access control for energy efficient transmission in cognitive radios. ArXiv e-prints*, (2014). http://arxiv.org/abs/1401.1671
13. R Hossain, R Rijul, MA Razzaque, MA Wadud, Prioritized medium access control in cognitive radio ad hoc networks: protocol and analysis. Wirel. Pers. Commun. **79**, 2383–2408 (2014)
14. K Liu, J Guo, N Lu, F Liu, *RAMC: A RSU-Assisted Multi-channel Coordination MAC Protocol for VANET*. (IEEE GLOBECOM Workshops, Hawaii, USA, 2009)
15. Y Zang, L Stibor, B Walke, H-J Reumerman, A Barroso, *A Novel MAC Protocol for Throughput Sensitive Applications in Vehicular Environments*. (IEEE, Vehicular Technology Conference, 2007)
16. Q Wang, S Leng, Y Zhang, H Fu, *A QoS Supported Multi-channel MAC for Vehicular Ad Hoc Networks*. (Vehicular Technology Conference, IEEE 73rd, Budapest, 2011), pp. 1–5
17. X Xie, B Huang, S Yang, T Lv, *Adaptive Multi-channel MAC protocol for dense VANET with Directional Antennas*. (Future Generation Communication IEEE conference, Hainan Island, China, 2008)
18. D Niyato, E Hossain, P Wang, Optimal channel access management with QoS support for cognitive vehicular networks. IEEE Trans. Mob. Comput. **10**(4), 573–591 (2011)
19. N Cheng, N Zhang, N Lu, X Shen, JW Mark, F Liu, Opportunistic spectrum access for CR-VANETs: a game-theoretic approach. IEEE T. Veh. Technol. **63**(1), 237–251 (2014)
20. Y Han, E Ekici, H Kremo, O Altintas, in *INFOCOM, 2014 Proceedings IEEE*. Throughput-efficient channel allocation in multi-channel cognitive vehicular networks, (2014), pp. 2724–2732
21. Z Lei, L Tao, L Wei, Z Siting, L Jianfeng, Cooperative spectrum allocation with QoS support in cognitive cooperative vehicular ad hoc networks. **11**(10), 49–59 (2014). Communications, China, IEEE
22. T Meng, F Wu, Z Yang, G Chen, A Vasilakos, Spatial reusability-aware routing in multi-hop wireless networks. IEEE Trans. Comput. **99**, 1–1
23. T Jiang, H Wang, AV Vasilakos, QoE-driven channel allocation schemes for multimedia transmission of priority-based secondary users over cognitive radio networks. IEEE J. Sel. Areas Commun. **30**(7), 1215–1224 (2012)
24. T Ycek, H Arslan, A survey of spectrum sensing algorithms for cognitive radio applications. IEEE Commun. Surv. Tutorials. **11**(1), 116–130 (2009)
25. M Subhedar, G Birajdar, *Spectrum sensing techniques in cognitive radio networks: a survey. International Journal of Next-Generation Networks*, vol. 3. (AIRCC Publishing Corporation, Chennai, Tamil Nadu, India, 2011)
26. D Cabric, A Tkachenko, RW Brodersen, Spectrum sensing measurements of pilot, energy, and collaborative detection. Washington DC, 2342–2348 (2006)
27. S Shobana, R Saravanan, R Muthaiah, Matched filter based spectrum sensing on cognitive radio for OFDM WLANs. International Journal of

Next-Generation Networks. **5**(1), 142–146 (2013). AIRCC Publishing Corporation, Chennai, Tamil Nadu, India

28. M Ghozzi, F Marx, M Dohler, J Palicot, in *1st International ICST Conference on Cognitive Radio Oriented Wireless Networks and Communications*. Cyclostatilonarilty-based test for detection of vacant frequency bands (IEEE, Mykonos Island, 2007), pp. 1–5
29. E-NS Youssef, SE El-Khamy, MS El-Mahallawy, in *Proceedings of the 2013 International Conference on Computing, Networking and Communications (ICNC)*. Improved wideband spectrum sensing techniques using wavelet-based edge detection for cognitive radio (IEEE Computer Society, San Diego, USA, 2013), pp. 418–423
30. H Hartenstein, KP Laberteaux, A tutorial survey on vehicular ad hoc networks. IEEE Commun. Mag. **46**, 164–171 (2008)
31. G Hasegawa, G Kang, Y Taniguchi, H Nakano, in *AICT 2011: The Seventh Advanced International Conference on Telecommunications*. Extending the protocol interference model considering sinr for wireless mesh networks (Think Mind, St. Maarten, The Netherlands Antilles, 2011), pp. 26–31
32. M Zorzi, RR Rao, Capture and retransmission control in mobile radio. IEEE J. Sel. Areas Commun. **12**, 1289–1298 (1994)
33. R Adhikari, RK Agrawal, An introductory study on time series modeling and forecasting. Comput. Res. Repository. **1302.6613**, 1–67 (2013)
34. X Li, SA Zekavat, in *IEEE Wireless Communications and Networking Conference*. Traffic pattern prediction and performance investigation for cognitive radio systems (IEEE, 2008), pp. 894–899
35. NEOS optimization server. http://www.neos-server.org/neos/, Accessed on 20 Sep, 2015.
36. The network simulator version 3 (NS-3). http://www.nsnam.org/, Accessed on 12 Sep, 2015
37. Simulation of Urban Mobility (SUMO) project. http://sumo.sourceforge.net/, Accessed on 11 Sep, 2015
38. M Youssef, M Ibrahim, M Abdelatif, L Chen, Routing metrics of cognitive radio networks: a survey. IEEE Commun. Surv. Tutorials. **16**(1), 92–109 (2014)